Journal of Sound and Vibration (1998) **210**(2), 255–265

BOLTED JOINT CLAMPING FORCE VARIATION DUE TO AXIAL VIBRATION

S. Basava and D. P. Hess

Department of Mechanical Engineering, University of South Florida, Tampa, FL 33620, *U.S.A.*

(*Received* 16 *July* 1997, *and in final form* 17 *September* 1997)

Recent experiments and analyses have revealed that threaded fasteners subjected to axial vibration can experience either loosening or tightening. In this paper, the authors examine the variation of clamping force in a single-bolt assembly model due to axial vibration. Specifically, the effect of vibration level and initial pre-load on clamping force is studied. It is found that the clamping force can remain steady, decrease, or increase when the assembly is subjected to axial vibration. However, changes in clamping force are generally transient and a steady value is reached over time.

1. INTRODUCTION

Threaded fasteners have found wide spread use in many machines and structures. Assemblies which utilize fasteners are often subjected to vibratory environments. Such conditions can lead to vibration-induced fastener loosening which can result in increased maintenance and/or failure.

Existing theories of the mechanism of vibration-induced loosening of threaded fasteners are based on static torque balances with supporting experimental data limited to low frequency conditions [1–3]. The basis of these theories is that friction holds a bolted joint together at a given clamping force, and vibration causes a reduction in friction which results in slip at the thread and head interfaces, and a reduction in clamping force.

Junker [1] proposed that bolts subjected to transverse vibrations become momentarily free of friction during each cycle of vibration and loosen. He showed that setting the thread and head coefficients of friction to zero in the static torque balance predicts loosening. Daadbin and Chow [4] modelled the elastic and damping characteristics of the thread interface of a simple bolt model and showed that the contact forces fluctuate, and are eliminated at separation, when the system is subjected to dynamic loading.

Experiments and analyses of threaded fasteners loaded by gravity and subjected to axial harmonic vibration revealed that threaded components can twist with or against gravity in the presence of vibration [5–6]. It was found that the applied vibration could be tuned such that either action occurs. The physical explanation for this observed behavior involves the non-linear dynamic interaction of the vibration and friction, and the resulting patterns of momentary sliding, sticking, and separation between the threaded components.

Hess and Sudhirkashyap [7] examined the dynamics of a moderately pre-loaded single-bolt assembly subjected to axial vibration. A broad range of vibration levels and frequencies were considered and both loosening and tightening behaviors were observed in experiments. A single-bolt assembly model was developed and simulations were performed for the first few cycles of applied vibration. This allowed the effect of various

0022–460X/98/070255 + 11 $25.00/0/sv981330

system parameters on initial loosening and tightening to be examined and compared with experimental observations.

In this paper, an improved version of the single-bolt assembly model introduced by Hess and Sudhirkashyap [7] is used to perform longer time simulations to examine changes in clamping force over time. In this work, a more realistic friction model is incorporated in the assembly model to more adequately accommodate complete stick. It is found that loosening or tightening, i.e., changes in clamping force, are generally transient and a steady value of clamping force is reached over time.

The focus in this paper is on axial vibration since ideally, bolted joints should be designed to carry static and dynamic loads axially. This is not always possible and the total load acting on a bolted joint is usually some combination of axial and transverse loads. The authors are currently studying assemblies subjected to transverse and combined transverse and axial vibrations.

2. MODEL

The single-bolt assembly consists of a bolt clamping a component to a base with a tapped hole. The dynamic model for this system can be visualized by unwrapping the threads of the tapped hole in the base and viewing them as upper and lower inclined constraints on the bolt threads, modelling the bolt as a lumped mass m_b constrained between the upper base threads and the clamped component, and modelling the clamped component as a lumped mass m_c constrained between the bolt head and the base. A sketch of this model is shown in Figure 1.

In the model the bolt is considered rigid with elastic interfaces. This model is sufficient for bolts with moderate pre-load as found in electronic equipment and joints with gaskets. One of the authors' current goals is to incorporate into the model both axial and torsional elastic bolt characteristics found in more heavily pre-loaded bolts.

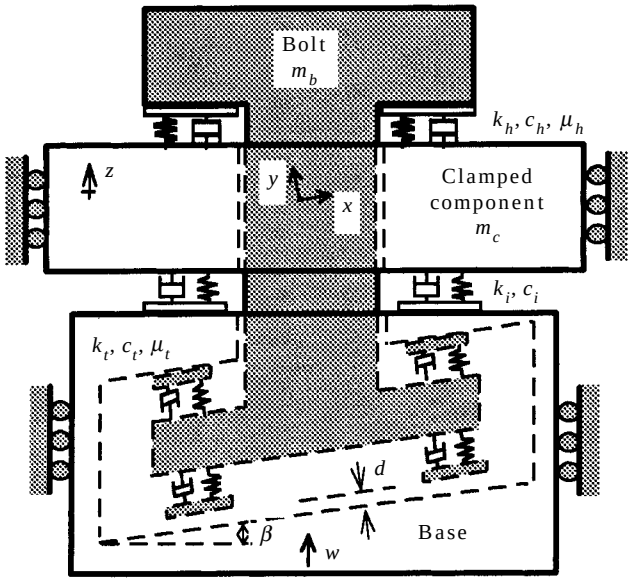

Figure 1. Dynamic model of the single-bolt assembly.

When in contact, the interfaces are modelled with elastic stiffness k_h, k_i, and k_t in parallel with dampers c_h, c_i, and c_t. Non-linear damping elements are used to avoid unrealistic discontinuous forces at the onset of contact and separation [8]. The friction forces at the thread interface and the bolt head interface are modelled with a friction model described below.

The system input and normal motion of the base is $w = w_0 \sin \omega t$. Co-ordinate z describes the normal motion of the clamped component. The co-ordinates x and y describe the motion of the bolt. Co-ordinate x represents the circular displacement of the bolt at the pitch diameter. This displacement is proportional to the turning angle $\theta = x/r_p$, where r_p is the pitch radius of the bolt. The lead angle of the bolt thread is β, and the thread clearance without pre-load is d_o. Note that an actual bolt system exhibits axial and rotational motion. The model described here represents an equivalent system in which the bolt can translate in two directions, x and y. This approach simplifies the model development considerably and is useful for studying the qualitative behavior of threaded fastener systems.

The equations of motion for this model depend on the relative positions of the bolt, the clamped component and the base. There exist six possible forms for the governing equations of the bolt and four possible forms for the clamped component. In one configuration, the bolt is in tension, the clamped component is in compression and all interfaces are in contact (see Figure 1). This condition is expressed mathematically as $(y - w\cos\beta) \geqslant -\delta_t$, $(y\cos\beta + x\sin\beta - z) \leqslant \delta_h$, $(z - w) \leqslant \delta_i$, where δ_t, δ_h and δ_i are the static deflections at the thread interface, bolt head and clamped component interface, and clamped component and base interface, respectively. The governing equations of motion for this configuration are

$$m_b \ddot{y} = -N_{tt} + N_h \cos\beta - F_h \sin\beta - m_b g \cos\beta, \tag{1}$$

$$m_b \ddot{x} = F_{tt} + N_h \sin\beta + F_h \cos\beta - m_b g \sin\beta, \qquad m_c \ddot{z} = -N_h + N_i - m_c g, \tag{2, 3}$$

where the normal contact forces are

$$N_h = (z + \delta_h - y\cos\beta - x\sin\beta)(k_h + c_h(\dot{z} - \dot{y}\cos\beta - \dot{x}\sin\beta)), \tag{4}$$

$$N_i = (w + \delta_i - z)(k_i + c_i(\dot{w} - \dot{z})),$$

$$N_{tt} = (y + \delta_t - w\cos\beta)(k_t + c_t(\dot{y} - \dot{w}\cos\beta)), \tag{5, 6}$$

and the static deflections are

$$\delta_h = \left(\frac{k_i\,\delta_i - m_c\,g}{k_h}\right), \qquad \delta_t = \left(\frac{k_h\,\delta_h - m_b\,g}{k_t}\right)\cos\beta, \tag{7, 8}$$

$$\delta_i = \frac{P}{k_i} - \left(\frac{(x - w\sin\beta)\sin\beta}{1 + k_i/k_h + k_i/k_t}\right), \tag{9}$$

where P is the initial pre-load in the joint. The clamping force is defined by $F_c = k_i\,\delta_i$. The thread interface friction force, F_{tt}, and the bolt head interface friction force, F_h, both oppose the circular sliding or twist of the bolt. The non-linear contact forces couple the axial motions of the system components with the twisting motion of the bolt.

The friction forces in the assembly are modelled with a friction model introduced by Karnopp [9]. The standard Coulomb friction model is discontinuous and has numerical limitations when the relative sliding velocities at the bolt thread and head interfaces approach zero. A number of friction models exist which remove these limitations (for an

excellent review see Armstrong *et al*. [10]), however, many of these models do not accommodate true stick. A friction model which includes stick and is both physically realistic and numerically manageable has been proposed by Karnopp [9]. This friction model defines a small velocity region between $-v_{min}$ and v_{min} surrounding zero sliding velocity. Inside this region, velocity is considered to be zero and the friction is determined by the forces acting on the system or by the friction breakaway value, whichever is less. Outside this region, friction is a function of velocity.

For the single-bolt assembly configuration in which the bolt is in tension, the clamped component is in compression and all interfaces are in contact (see Figure 1); there are friction forces at the bolt head and thread interfaces. To correctly determine the friction forces at these two interfaces, four cases must be considered: (1) both threads and head stick; (2) only threads stick; (3) only bolt head sticks; and (4) both threads and head slip. When both the threads and head stick, the friction force at the thread interface is

$$F_{tt} = \begin{cases} F_{tts}, & \text{for } |F_{tts}| < |\mu_{ts} N_{tt}|, \quad -v_{min} \leqslant (\dot{x} - \dot{w} \sin\beta) \leqslant v_{min}, \\ -\mu_{ts} N_{tt}, & \text{for } F_{tts} \leqslant -\mu_{ts} N_{tt}, \quad -v_{min} \leqslant (\dot{x} - \dot{w} \sin\beta) \leqslant v_{min}, \\ +\mu_{ts} N_{tt}, & \text{for } F_{tts} \geqslant +\mu_{ts} N_{tt}, \quad -v_{min} \leqslant (\dot{x} - \dot{w} \sin\beta) \leqslant v_{min}, \end{cases} \tag{10}$$

and the friction force at the bolt head interface is

$$F_h = \begin{cases} F_{hs}, & \text{for } |F_{hs}| < |\mu_{hs} N_h|, \quad -v_{min} \leqslant (\dot{x} \cos\beta - \dot{y} \sin\beta) \leqslant v_{min}, \\ -\mu_{hs} N_h, & \text{for } F_{hs} \leqslant -\mu_{hs} N_h, \quad -v_{min} \leqslant (\dot{x} \cos\beta - \dot{y} \sin\beta) \leqslant v_{min}, \\ +\mu_{hs} N_h, & \text{for } F_{hs} \geqslant +\mu_{hs} N_h, \quad -v_{min} \leqslant (\dot{x} \cos\beta - \dot{y} \sin\beta) \leqslant v_{min}, \end{cases} \tag{11}$$

where

$$F_{tts} = \left(\frac{1}{\sin\beta}\right)(m_b \ddot{w} - N_h + N_{tt} \cos\beta + m_b g), \qquad F_{hs} = -F_{tts} \cos\beta - N_{tt} \sin\beta, \tag{12, 13}$$

and μ_t, μ_{ts}, μ_h and μ_{hs} are the sliding and static coefficients of friction for the thread and head interfaces. When only the threads stick, the friction force at the bolt head interface is

$$F_h = \begin{cases} -\mu_h N_h, & \text{for } (\dot{x} \cos\beta - \dot{y} \sin\beta) > v_{min}, \\ +\mu_h N_h, & \text{for } (\dot{x} \cos\beta - \dot{y} \sin\beta) < -v_{min}, \end{cases} \tag{14}$$

and the friction force at the thread interface is

$$F_{tt} = \begin{cases} F_{tts}, & \text{for } |F_{tts}| < |\mu_{ts} N_{tt}|, \quad -v_{min} \leqslant (\dot{x} - \dot{w} \sin\beta) \leqslant v_{min}, \\ -\mu_{ts} N_{tt}, & \text{for } F_{tts} \leqslant -\mu_{ts} N_{tt}, \quad -v_{min} \leqslant (\dot{x} - \dot{w} \sin\beta) \leqslant v_{min}, \\ +\mu_{ts} N_{tt}, & \text{for } F_{tts} \geqslant +\mu_{ts} N_{tt}, \quad -v_{min} \leqslant (\dot{x} - \dot{w} \sin\beta) \leqslant v_{min}, \end{cases} \tag{15}$$

where

$$F_{tts} = m_b \ddot{w} \sin\beta - N_h \sin\beta - F_h \cos\beta + m_b g \sin\beta. \tag{16}$$

When only the bolt head sticks, the friction force at the thread interface is

$$F_{tt} = \begin{cases} -\mu_{ts} N_{tt}, & \text{for } (\dot{x} - \dot{w} \sin\beta) > v_{min}, \\ +\mu_{ts} N_{tt}, & \text{for } (\dot{x} - \dot{w} \sin\beta) < -v_{min}, \end{cases} \tag{17}$$

and the friction force at the bolt head interface is

$$F_h = \begin{cases} F_{hs}, & \text{for } |F_{hs}| < |\mu_{hs} N_h|, \quad -v_{min} \leqslant (\dot{x}\cos\beta - \dot{y}\sin\beta) \leqslant v_{min}, \\ -\mu_{hs} N_h, & \text{for } F_{hs} \leqslant -\mu_{hs} N_h, \quad -v_{min} \leqslant (\dot{x}\cos\beta - \dot{y}\sin\beta) \leqslant v_{min}, \\ +\mu_{hs} N_h, & \text{for } F_{hs} \geqslant +\mu_{hs} N_h, \quad -v_{min} \leqslant (\dot{x}\cos\beta - \dot{y}\sin\beta) \leqslant v_{min}, \end{cases} \tag{18}$$

where

$$F_{hs} = -F_{tt}\cos\beta - N_{tt}\sin\beta. \tag{19}$$

When both threads and head slip, the friction forces are defined by equations (14) and (17).

3. SYSTEM PARAMETERS

To examine the changes in clamping force resulting from vibration-induced loosening or tightening, the non-linear constrained equations of motion of the dynamic bolt assembly model are solved numerically using the fifth-order Runge–Kutta method.

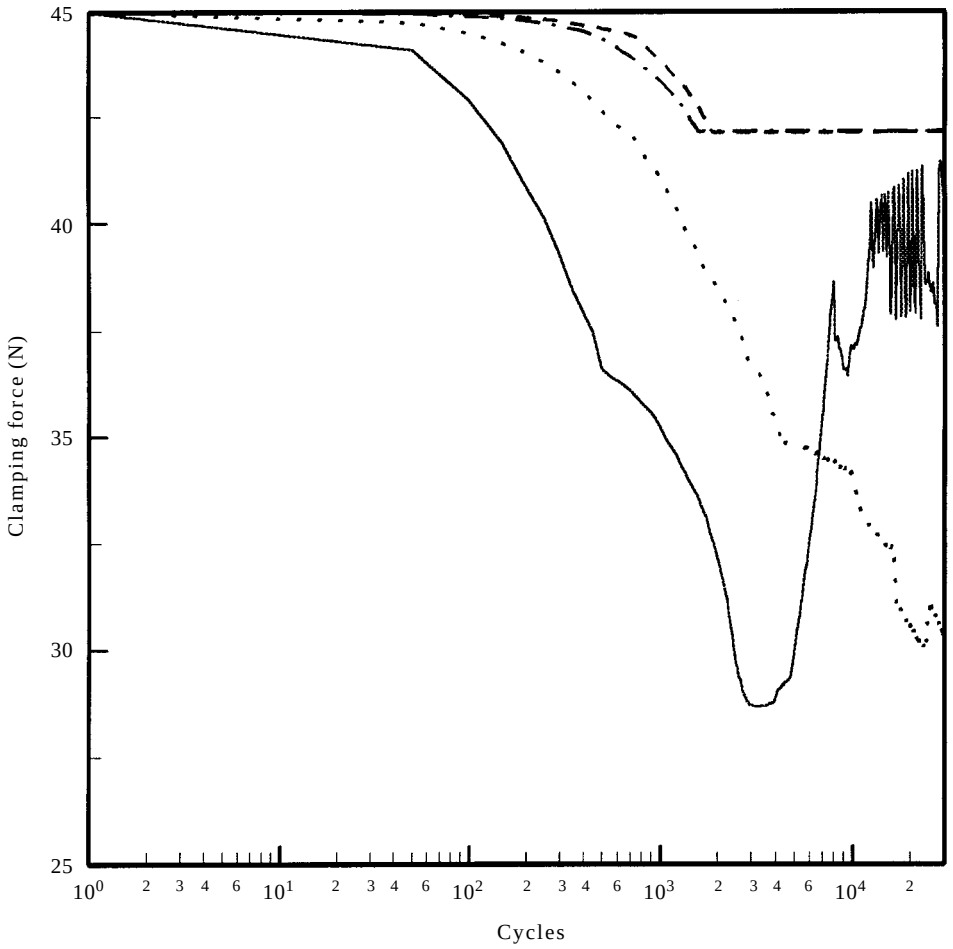

Figure 2. Effect of integration time-step: ——, 4×10^{-4} s; · · ·, 4×10^{-5} s; –·–·, 4×10^{-6} s; – – –, 4×10^{-7} s (pre-load of 45 N, acceleration level of 750 m/s^2 and v_{min} of 1×10^{-4} m/s).

The model parameters have been determined from a combination of direct measurement and estimation from acceleration measurements and bolt twist observations. The techniques used to determine the various system parameters have been described previously [6, 7]. For the simulation results presented in Figures 2–6, the parameters varied are the initial pre-load P, the input acceleration amplitude $\omega^2 w_o$, the integration time-step Δt, and the Karnopp velocity parameter v_{min}. The specific values for these parameters are given in each figure title. The remaining parameters, which are kept constant for all of these simulations, are $\omega = 2\pi(500)$ rad/s, $m_b = 0{\cdot}0096$ kg, $m_c = 0{\cdot}049$ kg, $k_h = 2{\cdot}025 \times 10^7$ N/m, $k_i = 7{\cdot}578 \times 10^4$ N/m, $k_t = 2{\cdot}80 \times 10^7$ N/m, $c_h = 8{\cdot}0 \times 10^6$ Ns/m^2, $c_i = 1{\cdot}80 \times 10^4$ Ns/m^2, $c_t = 1{\cdot}3 \times 10^8$ Ns/m^2, $\mu_h = \mu_t = 0{\cdot}2$, $\mu_{ts} = \mu_{hs} = 0{\cdot}22$, $r_p = 3{\cdot}17$ mm (0·125 in.), $\beta = 0{\cdot}05$ rad (2·87°), $d_o = 0{\cdot}015$ mm, and $g = 9{\cdot}81$ m/s^2.

Although Karnopp's friction model is known to be accurate for short time intervals, the accuracy of the technique for long intervals is unknown. As a result, it is necessary to examine the robustness of the simulation results to changes in the Karnopp velocity deadzone parameter v_{min} and the integration time-step Δt. Figure 2 provides representative simulations which illustrate the effect of the time-step on clamping force over a long time interval. Only small changes in the data are found when time-step intervals less than or

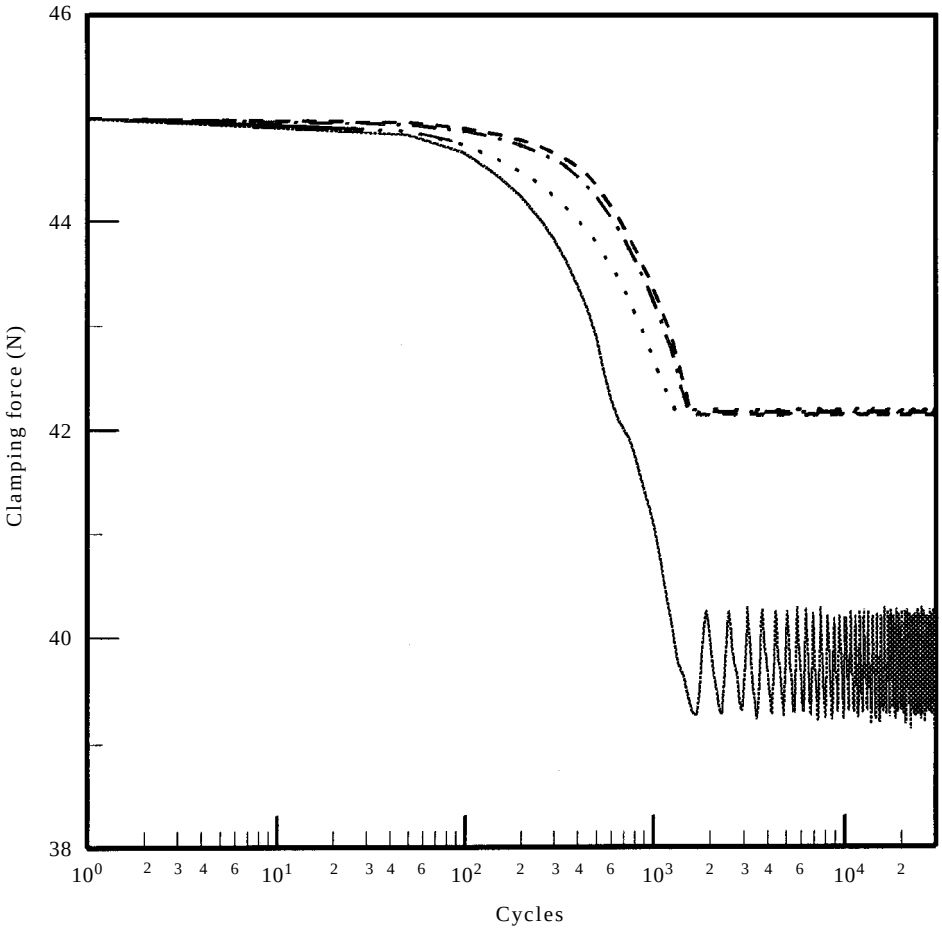

Figure 3. Effect of Karnopp deadzone parameter v_{min} : ——, 1×10^{-3} m/s; · · ·, 1×10^{-4} m/s; –·–·, 1×10^{-5} m/s; – – –, 4×10^{-9} s (pre-load of 45 N, acceleration level of 750 m/s^2 and Δt of 4×10^{-6} m/s).

equal to 4×10^{-6} s are used. The effect of the Karnopp deadzone parameter is shown in Figure 3. The data is quite consistent for values of v_{min} ranging from 10^{-4} to 10^{-9} m/s. However, for larger values a significant error accumulates over a large number of cycles. In an effort to minimize computer time while maintaining numerical accuracy, a time-step of 4×10^{-6} s and a Karnopp parameter v_{min} of 1×10^{-4} m/s are used in the simulations presented in this paper.

4. VARIATION IN CLAMPING FORCE

Before proceeding, it is worth summarizing the basic twisting behavior found by Hess and Sudhirkashyap [7]. At low levels of axial vibration, no twisting was observed. As the vibration level was increased, a loosening action occurred over a broad range of frequencies. As the vibration level was increased further, a tightening action developed at higher frequencies. In addition, it was found that changes in pre-load, component mass, input vibration frequency, or contact stiffness could cause a shift from one type of behavior to another. For example, for a given set of system parameters and vibration input level

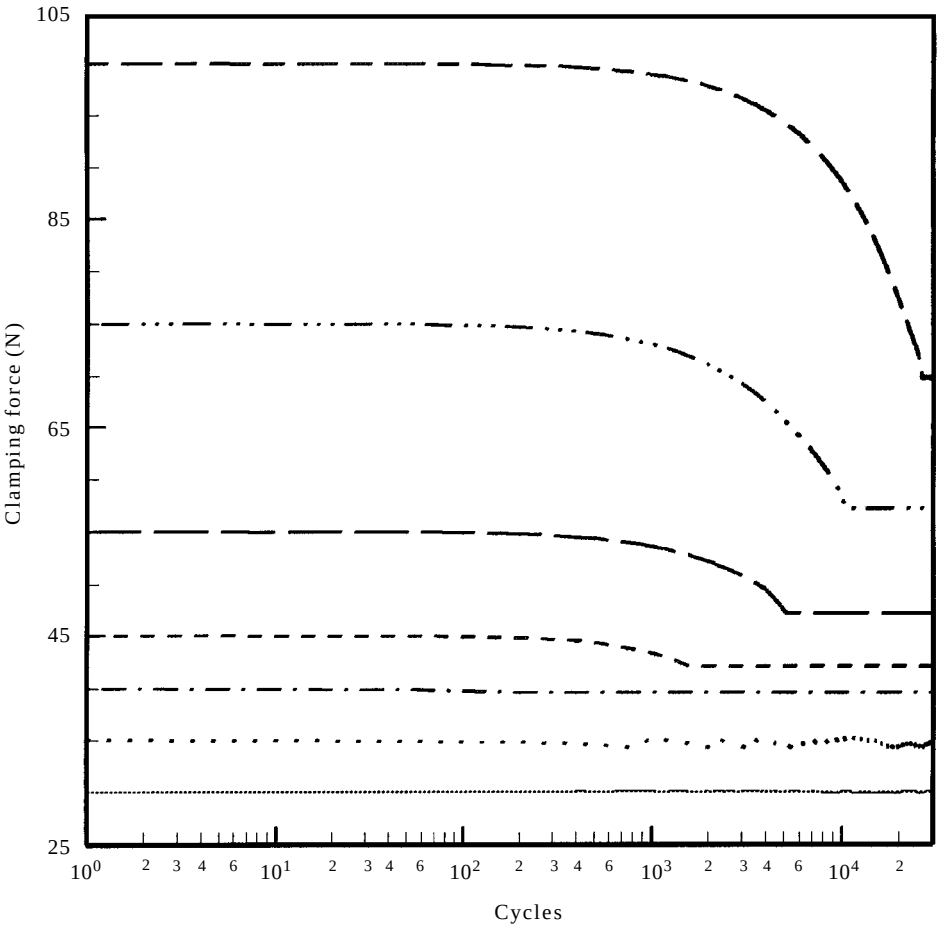

Figure 4. Loosening for different initial pre-loads: ——, 30 N; · · · , 35 N; –·–, 40 N; - - -, 45 N; ———, 55 N; – · · · –, 75 N; ———–, 100 N (acceleration level of 750 m/s^2, Δt of 4×10^{-6} s and v_{min} of 1×10^{-4} m/s).

and frequency, it was found that just varying the pre-load could result in a change from loosening to tightening.

The clamping force in the joint is found to remain steady for significant pre-loads and moderate vibration levels. As the pre-load decreases for a given vibration level, a transient reduction in clamping force occurs, but a steady value is reached over time. Figure 4 shows clamping force versus cycles of vibration for the single-bolt assembly pre-loaded from 30 to 100 N with an input vibration acceleration level of 750 m/s^2. The number of cycles to steady state decrease with pre-load. In addition, the amount of clamping force reduction decreases with pre-load. When the pre-load in the assembly is between 27 and 32 N, the clamping force remains steady or steady with small oscillatory fluctuations (e.g., see data for pre-load of 35 N).

As the pre-load is decreased from 30 N, the bolt actually tightens. Clamping force data for the single-bolt assembly pre-loaded from 12 to 30 N with an input vibration acceleration level of 750 m/s^2 are given in Figure 5. As the pre-load is decreased from 30 N, which gives a steady clamping force, the clamping force is found to increase. The number

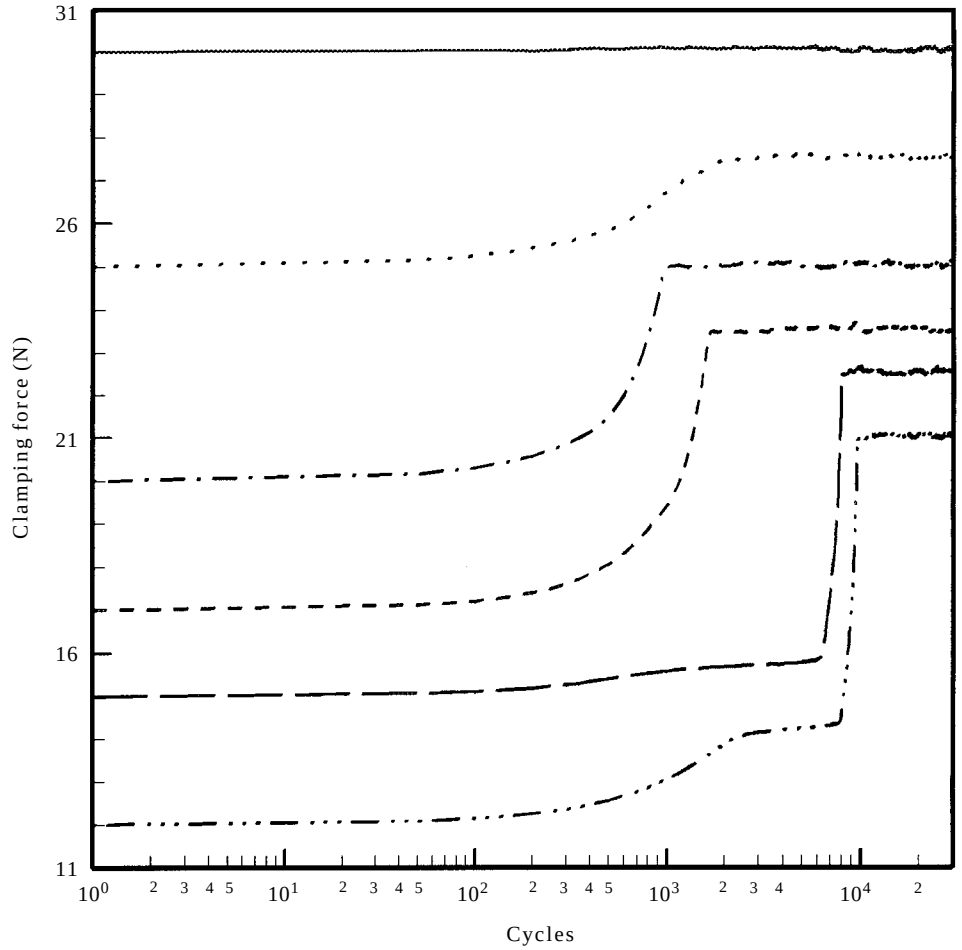

Figure 5. Tightening for different initial pre-loads: ——, 30 N; · · · , 25 N; —·—, 20 N; - - -, 17 N; ——, 15 N; —· · —· · , 12 N (acceleration level of 750 m/s^2, Δt of 4×10^{-6} s and v_{min} of 1×10^{-4} m/s).

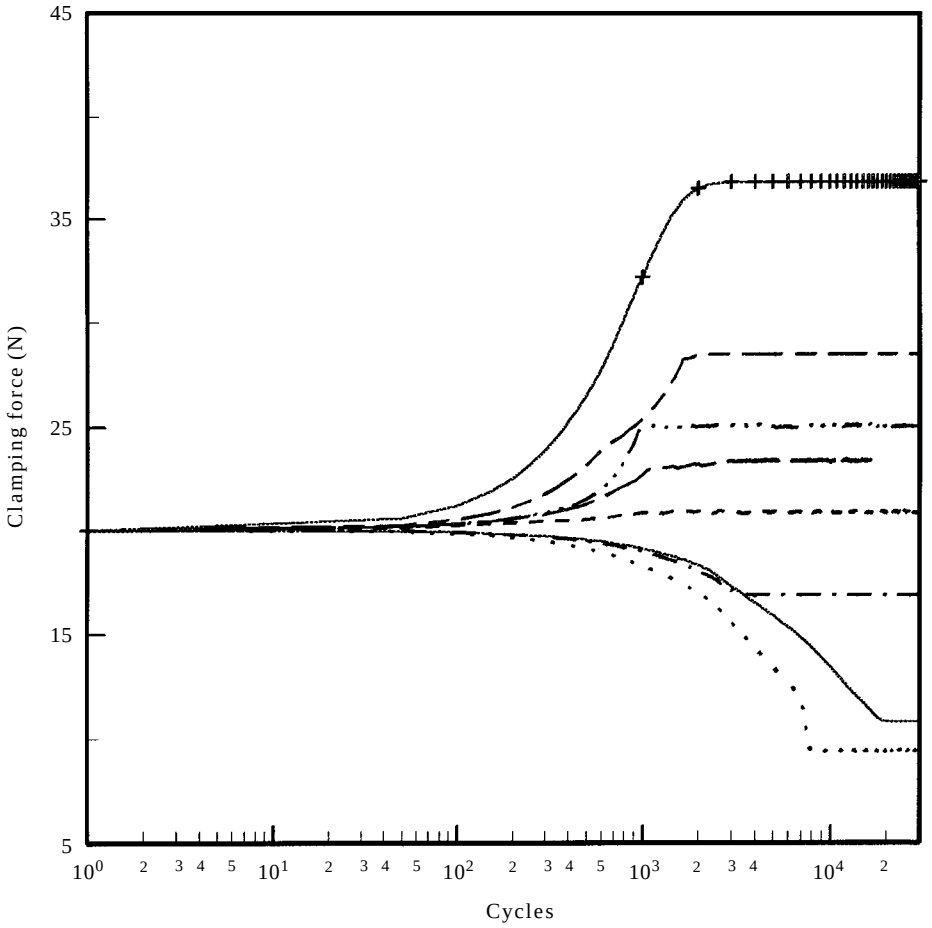

Figure 6. Clamping force versus cycles of vibration for different vibration acceleration levels : ——, 10 m/s^2; · · ·, 80 m/s^2; –·–·, 250 m/s^2; - - -, 500 m/s^2; ——, 600 m/s^2; –· · ·–· · ·, 750 m/s^2; — — —, 1000 m/s^2; – + –, 2000 m/s^2 (initial pre-load of 20 N, Δt of 4×10^{-6} s and v_{min} of 1×10^{-4} m/s).

of cycles necessary to reach a steady clamping force increases as the pre-load decreases. Also, the percentage increase in clamping force is found to increase as pre-load drops.

The effect of varying vibration level while keeping the initial pre-load constant has been examined. Figure 6 shows clamping force data for vibration levels ranging from 10 to 2000 m/s^2 with an initial pre-load of 20 N. Loosening is found for vibration levels below 250 m/s^2. As the vibration level is decreased from this value, the amount of clamping force loss increases until about 80 m/s^2. Below this level, the loss of clamping force decreases. The maximum percentage reduction in clamping force is 52·9%. Tightening occurs for vibration levels of 500 through 2000 m/s^2. At 2000 m/s^2 the percentage increase in clamping force is 83·4%. Simulations are currently being performed with higher vibration levels to determine whether the clamping force continues to increase with vibration level.

The steady state clamping force, percentage change in clamping force, and the number of cycles to steady state for the data in Figures 4 through 6 are given in Tables 1 and 2. Drops in clamping force by as much as 52·9% are found. Bickford [11] states that axial vibration can result in up to 40% reduction in clamping force, whereas transverse vibration can lead to complete loss of clamping force. This amount of reduction is 10% lower than

TABLE 1

Change in clamping force for different pre-loads with constant vibration level of 750 m/s^2

Pre-load (N)	Steady state clamping force (N)	Change in clamping force (%)	Cycles to steady state	Time to steady state (s)
12	21·014 ± 0·068	+75·1	15050	30·1
15	22·525 ± 0·075	+50·3	12500	25·0
17	23·490 ± 0·030	+38·2	1700	3·4
20	25·009 ± 0·007	+25·1	2000	4·0
25	27·479 ± 0·031	+11·0	2050	4·1
30	29·975 ± 0·025	0·0	0	0·0
35	34·760 ± 0·520	−0·7	150	0·3
40	39·640 ± 0·000	−1·0	200	0·4
45	42·135 ± 0·005	−6·4	1850	3·7
55	47·135 ± 0·005	−14·4	6800	13·6
75	57·135 ± 0·005	−23·9	15500	31·0
100	69·633 ± 0·004	−30·4	26650	53·3

what our simulations predict. Increases in clamping force by as much as 83·4% are also found. Although, significant amounts of loosening and tightening were observed in experiments with a single-bolt assembly apparatus [7], the maximum decrease and increase in clamping force possible from axial vibration were not determined.

This work and the data in Hess and Sudhirkashyap [7] suggest that substantial axial vibration levels are necessary to achieve an increase in clamping force. However, recent experiments show that lower levels of combined axial, transverse and angular vibration, as found in structures with bending, longitudinal and torsional modes of vibration, are necessary to achieve significant tightening [12]. For example, a vibration acceleration level of 25 $\boldsymbol{g}$ is capable of increasing the clamping force in a single-bolt joint on a cantilevered beam from 80 to 120 N.

4. CONCLUSIONS

Simulation of a single-bolt assembly model subjected to axial vibration have been performed to examine the variation of clamping force in the assembly due to the applied vibration. With high preloads and/or low vibration levels, the clamping force remains steady over a large number of cycles. As the pre-load decreases and/or the vibration level

TABLE 2

Change in clamping force for different vibration levels with constant pre-load of 20 *N*

Vibration level (m/s^2)	Steady state clamping force (N)	Change in clamping force (%)	Cycles to steady state	Time to steady state (s)
10	10·827 ± 0·001	−45·9	31250	62·5
80	9·423 ± 0·030	−52·9	12800	25·6
100	9·507 ± 0·573	−52·5	11350	22·7
250	16·868 ± 0·004	−15·7	5900	11·8
500	20·861 ± 0·861	+4·3	1250	2·5
600	23·306 ± 0·052	+16·5	2600	5·2
750	25·009 ± 0·007	+25·1	2000	4·0
1000	28·430 ± 0·007	+42·2	2150	4·3
2000	36·680 ± 0·009	+83·4	4350	8·7

increases, first loosening and then tightening of the assembly is found to occur. It is found that when loosening or tightening occurs, changes in clamping force are generally transient and a steady value is obtained with time. The model predicts that 52·9% is the maximum loss of clamping force possible from axial vibration. Increases in clamping force by as much as 83·4% are also found.

ACKNOWLEDGMENT

The authors gratefully acknowledge the support of the National Science Foundation under Grants CMS-9501824 and CMS-9629217.

REFERENCES

1. G. H. Junker 1969 *Society of Automotive Engineers Transactions* **78**, 314–335. New criteria for self-loosening of fasteners under vibration.
2. T. Sakai 1978 *Bulletin of JSME* **21**, 1385–1394. Investigations of bolt loosening mechanisms.
3. A. Yamamoto and S. Kasei 1984 *Bulletin of Japan Society of Precision Engineering* **18**, 261–266. A solution for self-loosening mechanism of threaded fasteners under transverse vibration.
4. A. Daadbin and Y. M. Chow 1992 *Mechanism and Machine Theory* **27**, 69–74. A theoretical model to study thread loosening.
5. D. P. Hess and K. D. Davis 1996 *ASME Journal of Vibration and Acoustics* **118**, 417–422. Threaded components under axial harmonic vibration: Part I. Experiments.
6. D. P. Hess 1996 *ASME Journal of Vibration and Acoustics* **118**, 423–429. Threaded components under axial harmonic vibration: Part II. Kinematic analysis.
7. D. P. Hess and S. Sudhirkashyap 1997 *ASME Journal of Vibration and Acoustics* **119**, 285–290. Dynamic loosening and tightening of a single-bolt assembly.
8. K. H. Hunt and F. R. Crossley 1975 *Journal of Applied Mechanics* **42**, 440–445. Coefficient of restitution interpreted as damping in vibro-impact.
9. D. Karnopp 1985 *ASME Journal of Dynamic Systems, Measurement, and Control* **107**, 100–103. Computer simulation of stick–slip friction in mechanical dynamic systems.
10. B. Armstrong-Helouvry, P. Dupont and C. C. Dewit 1994 *Automatica* **30**, 1083–1138. A survey of models, analysis tools and compensation methods for the control of machines with friction.
11. J. H. Bickford 1995 *An Introduction to the Design and Behavior of Bolted Joints*. New York: Marcel Dekker.
12. J. C. Peters 1996 *Thesis, University of South Florida*. Experiments on the interaction of structural dynamics and threaded fastener dynamics.